ISSN (Print) : 2320 – 3765
ISSN (Online): 2278 – 8875

International Journal of Advanced Research in Electrical, Electronics and Instrumentation Engineering

(An ISO 3297: 2007 Certified Organization)

Vol. 6, Issue 4, April 2017

Eigenvalue Loci of Small Signal Stability in Induction Motor

Nader barsoum*
Faculty of Engineering, University of Sabah, Malaysia

Abstract: This paper presents new loci of the eigenvalue which obtained from the characteristic equation of induction machine model represented in synchronous flux wave reference frame, which is time invariant frame. It discusses the inherent instability when the motor shaft is excited by small forced oscillation, and shows the analysis and the form of the dominant mode and the mode of causing the instability in the whole range of operating conditions. Stability analysis is investigated from the perturbation variables which relate to small signal model, and the eigenvalue loci is given by varying the important machine parameters within the range of operation.

Keywords: Principle reference frames; Perturbation; Dominant root; Model; Interchange mode

I. INTRODUCTION

When the induction drive is controlled by rectifier-inverter and controller [1], sometimes exhibits vibration and noise for few milliseconds and sometimes for longer period, and when is loaded at low speed sometimes it stop rotating and overheated [2], and also sometimes operates continuously without obeying the command of the controlled signal [3]. This could be happened due to stability problem in which the drive exhibits an inherent stability by itself and operates in different modes or different quadrants as related to the used inverter.

Stability has been investigated by many methods in the past [4-8] but the mode of operation to the stability is not yet examined at both low and high speeds. Inherent stability is investigated from perturbation variables which are linearly related to small signal analysis of electrical machines, when the shaft is excited by small forced oscillation with a small perturbation frequency [7]. Perturbation model in 2-axis form of induction motor is found to have time varying coefficients if expressed in stator or rotor reference frame, but it has time invariant coefficients if described in synchronous flux wave reference frame [4]. A particular study of stability problem in a machine is to investigate the locus of the eigenvalue of 2-axis machine represented in linear constant reference frame. Although this approach was used extensively its results are still not matched with the physical behavior in the whole region of operation, and in some conditions it was found a lack in appreciating the mode of dominant important and the mode of causing instability [6].

This paper, therefore, demonstrates most of the work developed in this area [5,6,8], and starts by describing the machine model in principle reference frames, then explains the characteristics of the eigenvalue with machine parameters in whole region of practical and not practically important. It shows the analytical formulae of dominant mode and the mode of causing instability in different regions of operating conditions.

II. SINGLE CAGE ROTOR INDUCTION MACHINE MODEL

2.1. 3-Phase/2-Phase Power Invariant Transformation

Sign convention: Many books in the literatures have ambiguity in defining the sign convention of 2-phase and 2-axis rotation, and the usual form found in the books is that the d-axis is in horizontal direction and q-axis is vertical, while phase *A* of 2-phase is aligned with phase *a* of 3-phase. This sometimes does not work with small signal analysis, especially when discussing the physical meaning of the results. Thus, a new form of sign convention is presented in this paper. As the stator 3-phase windings rotate with respect to the rotor in the direction *a-c-b* by velocity ω the 2 orthogonal coils in the stationary (non-pseudo stationary) frame rotates in the direction from *B* to *A*, corresponding to the 3-phase rotating windings. Therefore, the rotor is considered to be pseudo stationary, and the angle between phase *a* of 3-phase windings and phase *A* of the stationary 2 coil is considered to be the rotor position (θ), as shown in figure 1.

At θ = 0, phase *A* is aligned on phase *a*, and $v_a = v$ = maximum volt for this instance of time at ωt = 0, 180, 360, which makes phase *a* to conduct. This produces a maximum flux on the rotor, in which the induced *emf* at phase *A* is zero since

ISSN (Print) : 2320 – 3765
ISSN (Online): 2278 – 8875

International Journal of Advanced Research in Electrical, Electronics and Instrumentation Engineering

(An ISO 3297: 2007 Certified Organization)

Vol. 6, Issue 4, April 2017

$d\psi/dt$ = 0, while the maximum volt will be on phase *B* (90 ahead). For the next instance of time at ωt = 90, 270, … the voltage v_a = 0, consequently v_A is maximum corresponds to low flux and hence phase *B* has low voltage, attracting phase *a* at θ = 90. Therefore, the convenient sign convention for stationary reference frame is at θ = 90 and phase *B* lags *A* by 90, so that *B* is in the direction of phase *a*. This implies that the supply voltage to the stator is maximum on phase *B* at t = 0 (steady-state operation). Hence:

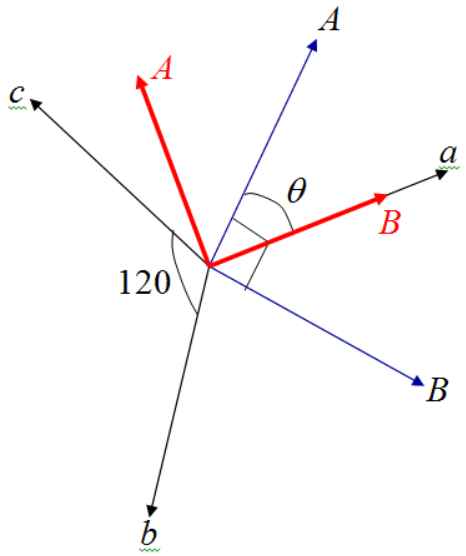

Figure 1: Phasor diagram of 3-phase 2-phase machine.

$v_B = v_a \angle \underline{0}$ $\quad v_A = v_{cb}/\sqrt{3} = (v_c - v_b)/\sqrt{3} = v_a \angle \underline{90}$ where the 3-phase voltages are:

$v_a = v\cos\omega t$ $\quad v_b = v\cos(\omega t - 120)$ $\quad v_c = v\cos(\omega t - 240)$ and the currents are:

$i_a = i\cos(\omega t - \varphi)$ $\quad i_b = i\cos(\omega t - 120 - \varphi)$ $\quad i_c = i\cos(\omega t + 120 - \varphi)$ for lagging power factor angle φ. *v* and *i* are the peak values of voltage and current respectively.

The transformation matrix for voltages can be obtained from figure 1 as in (1):

$$\begin{bmatrix} v_A \\ v_B \end{bmatrix} = \sqrt{\frac{2}{3}} \begin{bmatrix} \cos\theta & \cos(\theta+120) & \cos(\theta-120) \\ \sin\theta & \sin(\theta+120) & \sin(\theta-120) \end{bmatrix} \begin{bmatrix} v_a \\ v_b \\ v_c \end{bmatrix}$$ substitute for v_a, v_b, v_c therefore:

$$\begin{bmatrix} v_A \\ v_B \end{bmatrix} = \sqrt{\frac{3}{2}}\, v \begin{bmatrix} \cos(\omega t + \theta) \\ \sin(\omega t + \theta) \end{bmatrix} = \sqrt{\frac{3}{2}}\, v \begin{bmatrix} -\sin\omega t \\ \cos\omega t \end{bmatrix} \quad \text{at } \theta = 90 \qquad (1)$$

similarly for the currents: $\begin{bmatrix} i_A \\ i_B \end{bmatrix} = \sqrt{\frac{3}{2}}\, i \begin{bmatrix} -\sin(\omega t - \varphi) \\ \cos(\omega t - \varphi) \end{bmatrix}$ at $\theta = 90$

The coefficient $\sqrt{\frac{2}{3}}$ which appears in the transformation matrix is introduced in this paper for invariant power, where:

The 3-phase power = $P_3 = v_a i_a + v_b i_b + v_c i_c$

ISSN (Print) : 2320 – 3765
ISSN (Online): 2278 – 8875

International Journal of Advanced Research in Electrical, Electronics and Instrumentation Engineering

(An ISO 3297: 2007 Certified Organization)

Vol. 6, Issue 4, April 2017

$= vi\,[\cos\omega t \cos(\omega t - \varphi) + \cos(\omega t - 120)\cos(\omega t - 120 - \varphi) + \cos(\omega t + 120)\cos(\omega t + 120 - \varphi)] = \mathbf{(3/2)}\ \boldsymbol{vi}\ \mathbf{cos\varphi}$ (2)

The 2-phase power = $P_2 = v_A i_A + v_B i_B$

$= \sqrt{\frac{3}{2}}\, v \sqrt{\frac{3}{2}}\, i\,[-\sin\omega t\,(-\sin(\omega t - \varphi)) + \cos\omega t \cos(\omega t - \varphi)] = \mathbf{(3/2)}\ \boldsymbol{vi}\ \mathbf{cos\varphi}$ (3)

Thus, $P_3 = P_2$ from (2, 3). This means that they give an identical result when the transformation has the factor $\sqrt{\frac{2}{3}}$.

However, many books do not give correct transformation which resulted in different magnitude of transformed power by a value of 2/3.

2-phase squirrel cage induction motor variables

Since the rotor of squirrel cage motor is shorted then the rotor voltages are zero, while the rotor currents have rotor velocity Sω, where S is the slip. The stator voltage and current have relative velocity ω. The 2-phase variables, therefore, are given in (4):

Stator:	$v_{As} = -v \sin\omega t$	$i_{As} = -i_s \sin(\omega t - \varphi_s)$	
	$v_{Bs} = v \cos\omega t$	$i_{Bs} = i_s \cos(\omega t - \varphi_s)$	(4)
Rotor:	$v_{Ar} = 0$	$i_{Ar} = -i_r \sin(S\omega t - \varphi_r)$	
	$v_{Br} = 0$	$i_{Br} = i_r \cos(S\omega t - \varphi_r)$	

i_s and i_r and the corresponding φ_s, φ_r are the peak current and power factor angle of stator and rotor respectively

2.2. 2-Phase/2-Axis Transformation In Principle Reference Frames

Adjusting d-axis as a vertical and q-axis as horizontal to the right by 90 from d-axis, the 2-phase A and B makes an angle α with d and q respectively, in the positive direction of rotation from q to d, as shown in figure 2.

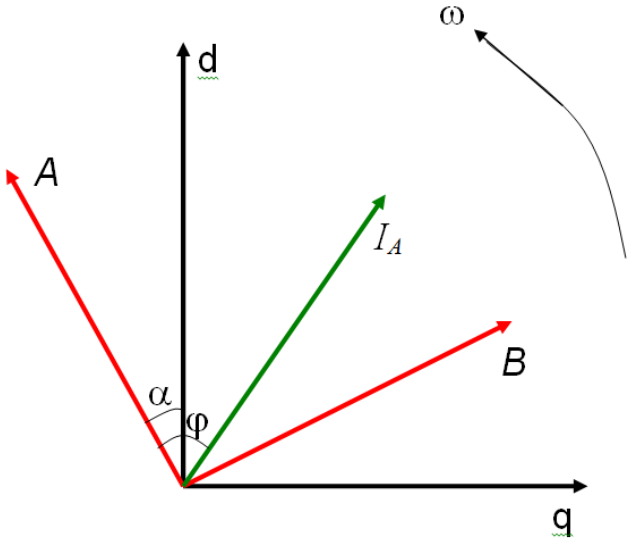

Figure 2: Phasor diagram of 2-phase 2-axis machine.

The orthogonal transformation is given in (5) from figure 2:

ISSN (Print) : 2320 – 3765
ISSN (Online): 2278 – 8875

International Journal of Advanced Research in Electrical, Electronics and Instrumentation Engineering

(An ISO 3297: 2007 Certified Organization)

Vol. 6, Issue 4, April 2017

$$\text{Stator} \quad \begin{bmatrix} v_{ds} \\ v_{qs} \end{bmatrix} = \begin{bmatrix} \cos\alpha & \sin\alpha \\ -\sin\alpha & \cos\alpha \end{bmatrix} \begin{bmatrix} v_{As} \\ v_{Bs} \end{bmatrix} \qquad \begin{bmatrix} i_{ds} \\ i_{qs} \end{bmatrix} = \begin{bmatrix} \cos\alpha & \sin\alpha \\ -\sin\alpha & \cos\alpha \end{bmatrix} \begin{bmatrix} i_{As} \\ i_{Bs} \end{bmatrix}$$

$$\text{Rotor} \quad \begin{bmatrix} v_{dr} \\ v_{qr} \end{bmatrix} = \begin{bmatrix} \cos\alpha & \sin\alpha \\ -\sin\alpha & \cos\alpha \end{bmatrix} \begin{bmatrix} v_{Ar} \\ v_{Br} \end{bmatrix} \qquad \begin{bmatrix} i_{dr} \\ i_{qr} \end{bmatrix} = \begin{bmatrix} \cos\alpha & \sin\alpha \\ -\sin\alpha & \cos\alpha \end{bmatrix} \begin{bmatrix} i_{Ar} \\ i_{Br} \end{bmatrix} \tag{5}$$

Where the angle α refers to the relative velocity between the member and frame, it is given in table 1.
It can be seen that α_s of stator member is 0 with respect to stator frame, ωt with synchronous frame and ω(1-S)t with rotor frame. Similarly α_r of rotor member is -ω(1-S)t with stator frame, Sωt with synchronous frame and 0 with respect to rotor frame. Flux and voltage equations in 2-axis forms for small signal variables (preceding by Δ) are given for 4-coil machine in (6):

Frame / Member	Stator	Rotor
Synchronous	ωt	Sωt
Stator	0	-ω(1-S)t
Rotor	ω(1-S)t	0

Table 1: Relative angle α of members in principle reference frames.

Flux forms

$$\psi_{ds} = L_s \Delta i_{ds} + M \Delta i_{dr}$$
$$\psi_{qs} = L_s \Delta i_{qs} + M \Delta i_{qr}$$
$$\psi_{dr} = L_r \Delta i_{dr} + M \Delta i_{ds}$$
$$\psi_{qr} = L_r \Delta i_{qr} + M \Delta i_{qs}$$

Perturbation voltage equations

$$\Delta v_{ds} = R_s \Delta i_{ds} + s\psi_{ds} - \psi_{qs} s\alpha_s$$
$$\Delta v_{qs} = R_s \Delta i_{qs} + s\psi_{qs} + \psi_{ds} s\alpha_s$$
$$\Delta v_{dr} = R_r \Delta i_{dr} + s\psi_{dr} - \psi_{qr} s\alpha_r \tag{6}$$
$$\Delta v_{qr} = R_r \Delta i_{qr} + s\psi_{qr} + \psi_{dr} s\alpha_r$$

where s denotes Laplace operator which represents the differential operator in time domain

Electric torque equation:

$$\Delta T_r = (\psi_{dr} + L_r i_{dr} + M i_{ds})(i_{qr} + \Delta i_{qr}) - (\psi_{qr} + L_r i_{qr} + M i_{qs})(i_{dr} + \Delta i_{dr}) \tag{7}$$
$$\text{or } \Delta T_r = M(i_{ds}\Delta i_{qr} + i_{qr}\Delta i_{ds} - i_{qs}\Delta i_{dr} - i_{dr}\Delta i_{qs})$$

Note that: i*i is steady-state term and Δi*Δi is second order of smallness term. Both terms are neglected. The mechanical torque is: $\Delta T_m = \Delta T_r + Js^2\alpha_r$ where *J* is the moment of inertia
By substituting for the flux into small signal voltage (6) and torque equations (7), the motional impedance matrix can now be written in the 3 principle reference frames as in (8), (9), (10):

Stator reference frame

$$\begin{bmatrix} -v\sin\omega t \\ v\cos\omega t \\ 0 \\ 0 \\ \Delta T_m \end{bmatrix} = \begin{bmatrix} R_s + L_s s & & Ms & & \\ & R_s + L_s s & & Ms & \\ Ms & M\omega(1-S) & R_r + L_r s & L_r\omega(1-S) & -\psi_{qr} \\ -M\omega(1-S) & Ms & -L_r\omega(1-S) & R_r + L_r s & \psi_{dr} \\ Mi_{qr} & -Mi_{dr} & -Mi_{qs} & Mi_{ds} & -Js \end{bmatrix} \begin{bmatrix} \Delta i_{ds} \\ \Delta i_{qs} \\ \Delta i_{dr} \\ \Delta i_{qr} \\ -\omega(1-S) \end{bmatrix} \tag{8}$$

ISSN (Print) : 2320 – 3765
ISSN (Online): 2278 – 8875

International Journal of Advanced Research in Electrical, Electronics and Instrumentation Engineering

(An ISO 3297: 2007 Certified Organization)

Vol. 6, Issue 4, April 2017

Rotor reference frame

$$\begin{bmatrix} -v\sin S\omega t \\ v\cos S\omega t \\ 0 \\ 0 \\ -\Delta T_m \end{bmatrix} = \begin{bmatrix} R_s + L_s s & -L_s\omega(1-S) & Ms & -M\omega(1-S) & -\psi_{qs} \\ L_s\omega(1-S) & R_s + L_s s & M\omega(1-S) & Ms & \psi_{ds} \\ Ms & & R_r + L_r s & & \\ & Ms & & R_r + L_r s & \\ -Mi_{qr} & Mi_{dr} & Mi_{qs} & -Mi_{ds} & -Js \end{bmatrix} \begin{bmatrix} \Delta i_{ds} \\ \Delta i_{qs} \\ \Delta i_{dr} \\ \Delta i_{qr} \\ \omega(1-S) \end{bmatrix} \quad (9)$$

Synchronous flux wave reference frame

$$\begin{bmatrix} 0 \\ v \\ 0 \\ 0 \\ \Delta T_m \end{bmatrix} = \begin{bmatrix} R_s + L_s s & -L_s\omega & Ms & -M\omega & \\ L_s\omega & R_s + L_s s & M\omega & Ms & \\ Ms & -MS\omega & R_r + L_r s & -L_r S\omega & -\psi_{qr} \\ MS\omega & Ms & L_r S\omega & R_r + L_r s & \psi_{dr} \\ Mi_{qr} & -Mi_{dr} & -Mi_{qs} & Mi_{ds} & -Js \end{bmatrix} \begin{bmatrix} \Delta i_{ds} \\ \Delta i_{qs} \\ \Delta i_{dr} \\ \Delta i_{qr} \\ S\omega \end{bmatrix} \quad (10)$$

The 4 steady state currents are given in terms of machine parameters and v in the appendix.
It can be seen that the voltage vector is variable in both models of stator and rotor frames while it is constant in synchronous frame

III. CHARACTERISTIC EQUATION

From the machine model of autonomous system with time invariant coefficients related to the synchronous reference frame, the characteristic equation is the determinant of the motional impedance matrix (10). Consideration is emphasized on the physical behavior that the machine is capable of inherent stability, essentially because the internal electromechanical topology can be represented as a multiple closed loop system. This closed loop nature drawing attention to a particular important feedback path through the oscillation of the shaft is focused by mathematically depicting the machine in the form of a chosen transfer function with torque perturbation as input and shaft speed as output. The block diagram is given in figure 3.

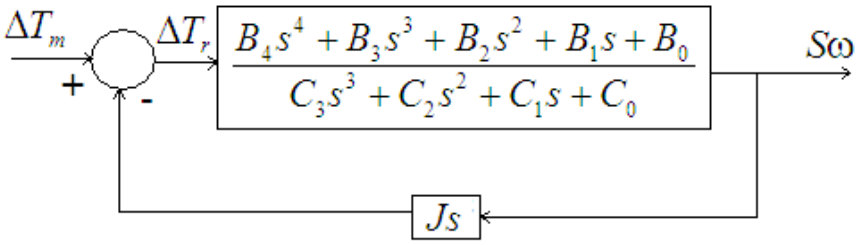

Figure 3: Block diagram of dynamic machine.

The characteristic equation is given in (11):

$$B_4 s^5 + B_3 s^4 + (B_2 + C_3/J)s^3 + (B_1 + C_2/J)s^2 + (B_0 + C_1/J)s + C_0/J = 0 \quad (11)$$

This is 5th order or polynomial of degree 5, where B's and C's are given in the appendix in terms of machine parameters. The eigenvalue are the roots of this equation, so that there are 5 roots (one real root and 2 pairs of complex conjugate).

ISSN (Print) : 2320 – 3765
ISSN (Online): 2278 – 8875

International Journal of Advanced Research in Electrical, Electronics and Instrumentation Engineering

(An ISO 3297: 2007 Certified Organization)

Vol. 6, Issue 4, April 2017

Referring to the characteristic equation of figure 3, particular solution of the eigenvalue and detailed explanation with the parameters are followed and then proceeds to the general behavior of the root loci. Stability and the dominant mode are observed by selecting important parameters like stator and rotor resistances, R_s and R_r, excitation frequency ω, and the feedback parameter J, the moment of inertia.

IV. VARIATION OF RESISTANCES FROM ZERO

When all resistances are made zero (no losses) some interesting behavior of the eigenvalue are observed. The state space system matrix has zero main diagonal and becomes skew symmetric. This case naturally gives zero damped eigenvalue and the characteristic equation reduces to the form of (12)

$$s(s^4 + \omega^2(1+S^2)s^2 + S^2\omega^4) = 0 \qquad (12)$$

The solution is: $s_{1,2} = \pm j\omega \qquad s_{3,4} = \pm jS\omega \qquad s_5 = 0$

At zero resistances the 2 pairs of eigenvalue are exactly the stator and rotor velocities, respectively. Thus, they are independent of J and all impedances but however, under some circumstances, this solution is found to be a discontinuous result, in the sense that for resistances non-zero but tending to zero, root loci do not tend to the value $\pm jS\omega$. They tend instead to $\pm j\frac{\sqrt{\eta}}{\omega}$, where $\eta = \frac{1}{JL_sL_s^{"}}$, where L_s is stator self-inductance and $L_s^{"}$ is the sub transient inductance.

When the machine operates at no load (S = 0) the second $s_{3,4}$ pair is $\pm j\frac{\sqrt{\eta}}{\omega}$ as resistances tend to zero, but jumps discontinuously to zero when the resistances are exactly zero, and then to $\pm jS\omega$ when the machine is loaded. This behavior is understandable and does not represent a physically important effect. In the limit, it is believed that the solution is actually indeterminate in the same way that even the steady state torque is indeterminate when rotor resistance is zero. When the slip is not zero, the solution at zero resistances is determinate = $\pm jS\omega$. This is confirmed by experience that shows root loci tending to $\pm j\frac{\sqrt{\eta}}{\omega}$ as resistances tend to zero, and equal to $\pm jS\omega$ in the limit.

When the stator resistance R_s alone is increased from zero and for any value of J, it is observed that the first pair $s_{1,2}$ of roots rapidly becomes highly positively damped, whilst its frequency remains (at least for typical values of machine parameters) approximately ω. The second pair $s_{3,4}$ immediately jumps in frequency from $S\omega$ to $\frac{\sqrt{\eta}}{\omega}$ because of the discontinuous property, but the degree of damping varies in a complicated manner depend on J. Instability (i.e. negative damping) may occur in this condition. Alternatively, when the rotor resistance R_r alone is increased from zero, it is observed that the first pair of roots remains almost exactly at frequency ω with very slight damping. The second pair remains approximately at frequency $\frac{\sqrt{\eta}}{\omega}$ and again exhibits complicated behavior in damping depend upon J, which may be positive or negative. With $1/J = 0$, however, the second pair is strongly positively damped.

When both resistances are raised simultaneously from zero, the behavior may still show some simple features for typical ranges of machine parameters. The first pair is observed to be positively damped, through of damping may be high or low, dependent upon all machine parameters including J. The second pair however, is observed to be unstable for particular range of machine parameters with complicated dependence. It is believed, and the evident of the work suggest, that the first

ISSN (Print) : 2320 – 3765
ISSN (Online): 2278 – 8875

International Journal of Advanced Research in Electrical, Electronics and Instrumentation Engineering

(An ISO 3297: 2007 Certified Organization)

Vol. 6, Issue 4, April 2017

pair is always stable, and instability is always due to the second pair. All the preceding discussion is illustrated in figures 4-9.

V. VARIATION OF 1/*J* FROM ZERO

Consider the case $1/J = 0$, the characteristic equation (11) reduces to the form of (13)

$$(k_4 s^2 + k_1 s + R_s R_r)^2 + (k_4 s + R_r L_s)^2 \omega^2 = 0 \qquad \text{at zero slip} \qquad (13)$$

where k_1 and k_4 are given in the appendix. The solution is:

$$s_{1,2} = -\frac{1}{2}[(\frac{k_1}{k_4} \pm j\omega) \pm \sqrt{(\frac{k_1}{k_4} \pm j\omega)^2 - \frac{4R_r}{k_4}(R_r + j\omega L_s)}]$$
$$s_{3,4} = -\frac{1}{2}[(\frac{k_1}{k_4} \pm j\omega) \pm \sqrt{(\frac{R_s L_r - R_r L_s}{k_4} \pm j\omega)^2 + \frac{4R_s R_r M^2}{k_4^2}}] \qquad (14)$$

If $R_s = 0$, then $s_{1,2} = \pm j\omega \qquad s_{3,4} = -\frac{R_r L_s}{k_4}$ (15)

imaginary pair at ω, and a repeated root with rotor (or sub transient) time constant

If $R_r = 0$, then $s_{1,2} = -(\frac{R_s L_r}{k_4} \pm j\omega) \qquad s_{3,4} = 0$ (16)

A pair at ω with armature time constant and pair at origin

VI. INTERCHANGE OF MODES IN THE 2-AXIS MACHINE

For the 2 complex modes of induction motor, the mode originating with zero resistances from $\pm j\omega$ is recognizably due primarily to the stator winding, its time constant with only non-zero R_s being (exactly under the condition of zero slip and zero $1/J$) the armature time constant, as seen from (16). Equally the mode asymptotic to $\frac{\sqrt{\eta}}{\omega}$ is recognizably due primarily to the rotor winding, the time constant with only non-zero R_r being sub transient, as in (15).

It is interested to plot the loci of these 2 modes, for various combination of machine parameters, as a two stage process; in the first stage the resistances are raised from zero to set their values at zero $1/J$, and in the second stage $1/J$ is raised from zero to infinity. By this procedure, one is enable to 'keep track' of the stator and rotor modes, and identify them in all circumstances. Figures 4-11 show this procedure.

A remarkable behavior is exhibited, for example, when ω is low (= 0.2 pu) and the ratio of stator to rotor resistances is varied, it concerns a root which is dominant in the range of $1/J$ for which the machine is either very highly damped or unstable. In this case, when R_s is sufficiently large relative to R_r, the rotor mode is dominant; but with R_s small an interchange of mode occurs in rather dramatic fashion and the stator mode becomes dominant. In all author's experience, while the rotor mode can readily be unstable, the stator mode is never observed to be so, although very high damped. Figures 4-9 demonstrate this behavior. Thus, either mode can be dominant.

With ω sufficiently high (= 0.6 pu), the rotor mode may become dominant in a range of $1/J$, and may be unstable as figure 10 shows. This leads to a high ω region of instability observed on D-partition diagrams [6].

The interchange behavior of the root loci may occur either in the resistance range at zero $1/J$ or in the subsequent $1/J$ range. In the first case it is interesting to observe that an exact solution can be obtained, with which to explore the effect. At S = 0 and by factorizing the characteristic equation with $1/J = 0$, the 2 pairs of complex roots are seen to have the form (14). In this expression, the first and third sign-alternatives (±) generate the complex conjugates, and the second generates the two distinct pairs of root. Interchange occurs precisely when the pairs are equal, i.e. the square root is zero. This needs two conditions to be satisfied, which are:

ISSN (Print) : 2320 – 3765
ISSN (Online): 2278 – 8875

International Journal of Advanced Research in Electrical, Electronics and Instrumentation Engineering

(An ISO 3297: 2007 Certified Organization)

Vol. 6, Issue 4, April 2017

$$R_sL_r = R_rL_s \qquad \text{condition 1}$$

$$4R_sR_rM^2 = \omega^2(L_sL_r - M^2)^2 \qquad \text{condition 2}$$

The behavior shown in figure 6, for example, exactly agrees with these conditions.
It emerges from other figures 10,11 which show interchange within the $1/J$-range of loci, that the general form of the solution for the root pairs is probably still as above when $1/J$ is not zero, although modified in the constituent terms. As seen in figures 5,7 interchange can occur when $1/J > 0$, but under the conditions that do not even approximate to condition 1 and condition 2.

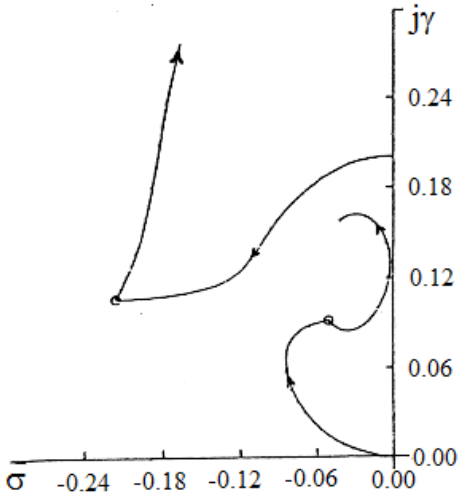

Figure 4: Eigenvalue loci for $R_s > R_r$ at $\omega = 0.2$, $S = 0$ and $(1/J)_{start} = 0$.

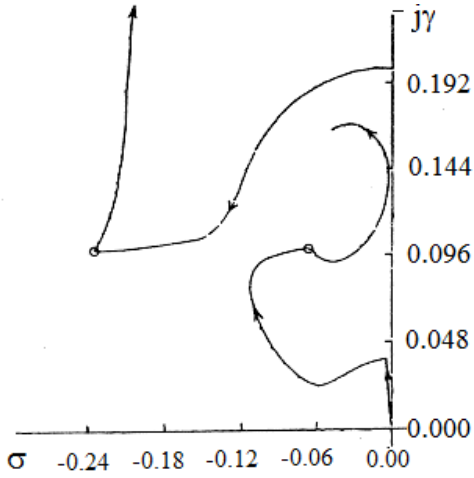

Figure 5: Eigenvalue loci for $R_s > R_r$ at $\omega = 0.2$, $S = 0$ and $(1/J)_{start} = 10^{-1}$.

ISSN (Print) : 2320 – 3765
ISSN (Online): 2278 – 8875

International Journal of Advanced Research in Electrical, Electronics and Instrumentation Engineering

(An ISO 3297: 2007 Certified Organization)

Vol. 6, Issue 4, April 2017

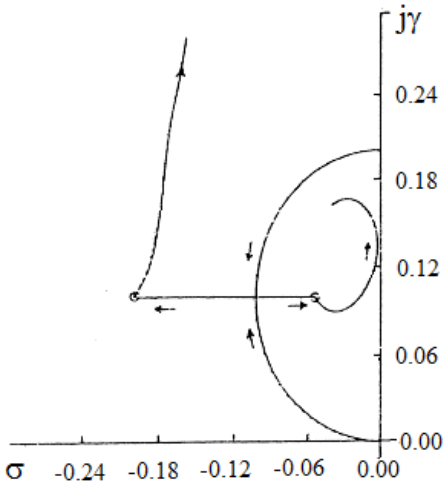

Figure 6: Eigenvalue loci for $R_s = R_r$ at ω = 0.2, S = 0 and $(1/J)_{start}$ = 0.

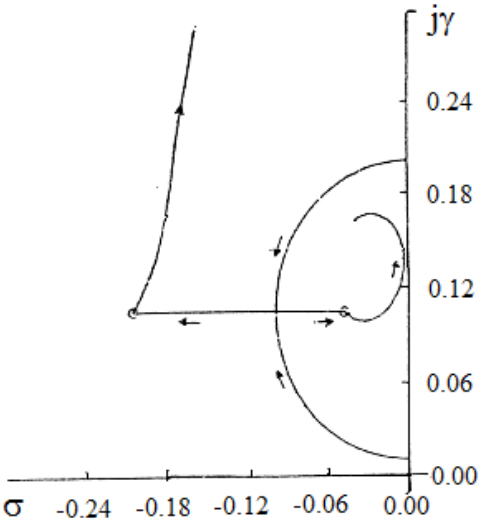

Figure 7: Eigenvalue loci for $R_s = R_r$ at ω = 0.2, S = 0.05 and $(1/J)_{start}$ = 0.

ISSN (Print) : 2320 – 3765
ISSN (Online): 2278 – 8875

International Journal of Advanced Research in Electrical, Electronics and Instrumentation Engineering

(An ISO 3297: 2007 Certified Organization)

Vol. 6, Issue 4, April 2017

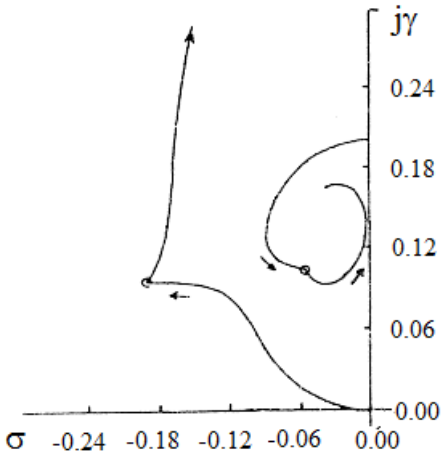

Figure 8: Eigenvalue loci for $R_s < R_r$ at $\omega = 0.2$, $S = 0$ and $(1/J)_{start} = 0$.

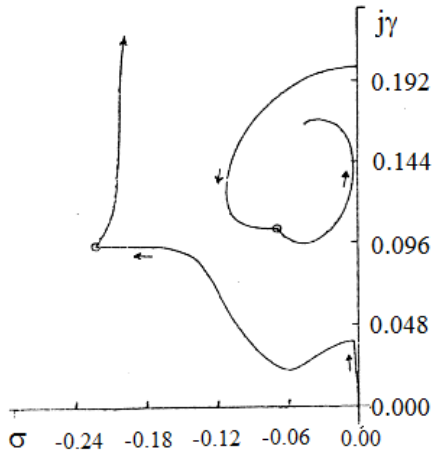

Figure 9: Eigenvalue loci for $R_s < R_r$ at $\omega = 0.2$, $S = 0$ and $(1/J)_{start} = 10^{-1}$.

ISSN (Print) : 2320 – 3765
ISSN (Online): 2278 – 8875

International Journal of Advanced Research in Electrical, Electronics and Instrumentation Engineering

(An ISO 3297: 2007 Certified Organization)

Vol. 6, Issue 4, April 2017

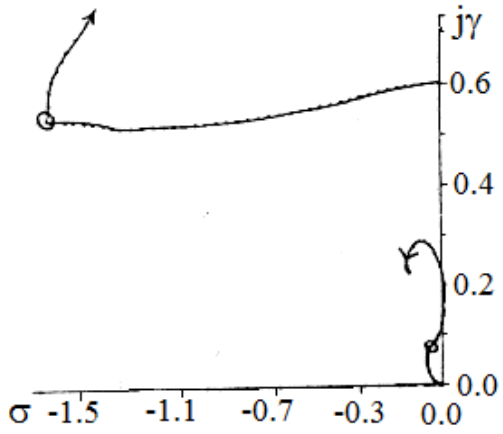

Figure 10: Eigenvalue loci for $R_s >> R_r$ at $\omega = 0.6$, $S = 0$ and $(1/J)_{start} = 0$.

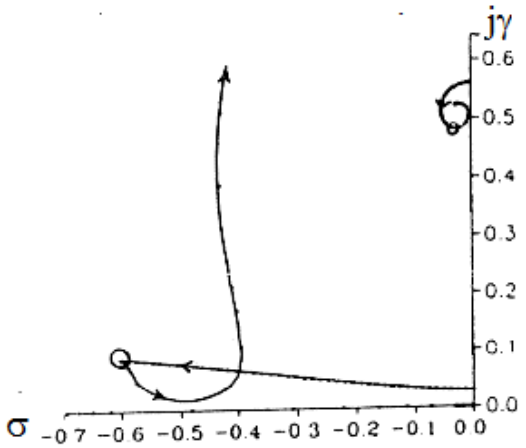

Figure 11: Eigenvalue loci for $R_s << R_r$ at $\omega = 0.6$, $S = 0.05$ and $(1/J)_{start} = 10^{-1}$.

VII. CONCLUSION

The 2-axis induction motor model for perturbation variables is presented in three principle reference frames. Behaviors of eigenvalues for machine model in autonomous reference frame are illustrated. A wider range of exact solution is found, corresponding to restricted special conditions. Eigenvalue loci are drawn for successive variation of two machine parameters, so as to permit roots to be tentatively labeled 'stator' and 'rotor'. Intersecting phenomena are noted concerning rapid interchange of root positions in the complex plane, and it appears likely that a 'stator' root pair may be lightly damped but is always stable, whereas a 'rotor' root pair may be dynamically unstable.

In general, induction motor includes 2 pairs of complex eigenvalue and one real for usual value of machine parameters. Only one pair may be unstable, which is always imaginary (oscillatory) on the stability boundary. Static instability, when it occurs, is represented by a single real root. No further root can be unstable.

ISSN (Print) : 2320 – 3765
ISSN (Online): 2278 – 8875

International Journal of Advanced Research in Electrical, Electronics and Instrumentation Engineering

(An ISO 3297: 2007 Certified Organization)

Vol. 6, Issue 4, April 2017

REFERENCES

1. Barsoum NN, Harris MR, Theorems of torque coefficients on stability for induction and reluctance machines, International Journal of electrical engineering education IJEEE, Manchester institute of science and technology UMIST, UK 2001; 38: 260-275
2. Barsoum N, Performance of Direct Torque Control Implemented in Speed Drive. Global Journal of Technology and Optimization GJTO 2012; 3: 59-64.
3. Barsoum N, Pin RC, Internet Control Drive Project using Lab View via PLC. Journal of Intelligent Control and Automation, November 2011; 2.
4. Barsoum N, Speed Control of the Induction Drive by Temperature and Light Sensors via PIC, Global Journal of Technology and Optimization GJTO 2010; 1: 53-59.
5. Barsoum NN, Time Domain Transfer Function of the Induction Motor. Journal of Studies in Engineering and Technology 2014; 1: 1-9.
6. Barsoum NN, Characteristics and properties of small signal electrical machine stability, Journal of institution of engineers, Calcutta, India 1998; 79: 66-71.
7. Barsoum NN, Nagrial M, Small signal stability of reluctance synchronous machines, Proceeding of Australian universities in power and energy conference AUPEC'97, NSW, Sydney 29/9-1/10 1997; 1: 205-210.
8. Barsoum NN, Equivalent circuits and torque components in true variables for the induction motor', Alexandria Engineering Journal AEJ, Egypt 1991; 30: 13-28.